Forces in Mechanics 9 (2022) 100143

Contents lists available at ScienceDirect

Forces in Mechanics

journal homepage: www.sciencedirect.com/journal/forces-in-mechanics

Evaluating the predictive character of the method of constrained geometries simulate external force with density functional theory

Christian R. Wick [a,c,*], Ece Topraksal [a], David M. Smith [b], Ana-Sunčana Smith [a,b,*]

[a] Friedrich-Alexander-Universität Erlangen-Nürnberg (FAU), Institute for Theoretical Physics, PULS Group, Interdisciplinary Center for Nanostructured Films (IZNF), Cauerstrasse 3, Erlangen 91058, Germany
[b] Group for Computational Life Sciences, Division of Physical Chemistry, Ruđer Bošković Institute, Bijenička cesta 54, Zagreb 10000, Croatia
[c] Friedrich-Alexander-Universität Erlangen-Nürnberg (FAU), Competence Unit for Scientific Computing (CSC), Martensstr. 5a, Erlangen 91058, Germany

ARTICLE INFO

Keywords:
COGEF
Density Functional Theory (DFT)
Mechanical force
Mechanochemistry
Molecular fracture
Mechanical bond scission
Mechanoradicals

ABSTRACT

Mechanochemistry is a fast-developing field of interdisciplinary research with a growing number of applications. Therefore, many theoretical methods have been developed to quickly predict the outcome of mechanically induced reactions. Constrained geometries simulate External Force (CoGEF) is one of the earlier methods in this field. It is easily implemented and can be conducted with most DFT codes. However, recently, we observed totally different predictions for model systems of epoxy resins in different conformations and with different density functionals. To better understand the conformational and functional dependence in typical CoGEF calculations we present a systematic evaluation of the CoGEF method for different model systems covering homolytic and heterolytic bond cleavage reactions, electrocyclic ring opening reactions and scission of non-covalent interactions in hydrogen-bond complexes. From our calculations we observe that many mechanochemical descriptors strongly depend on the functional used, however, a systematic trend exists for the relative maximum Force. In general, we observe that the CoGEF procedure is forcing the system to high energetic regions on the molecular potential energy profiles, which can lead to unexpected and uncorrelated predictions of mechanochemical reactions. This is questioning the true predictive character of the method.

Introduction

It is well understood that mechanical forces induce versatile chemical reactions in polymeric materials at the molecular scale [1–5]. The types of reactions that can be triggered by mechanical energy range from simple heterolytic or homolytic bond breaking to unexpected and otherwise forbidden chemical reactions [3,4,6,7]. This opened up the field for synthesis of compounds with predetermined mechanochemical reactivity, so-called mechanophores [2,8–10]. However, the prediction of mechanochemical reactivity of polymer chains or mechanophores is very difficult by experimental means, so that computational methods became indispensable to investigate the induction of chemical reactivity by mechanical force and to streamline the design of new mechanophoric components [11–15]. While most computational methods that allow incorporation of an external force afford a priori knowledge of the expected reaction mechanism, the Constrained Geometries Simulate External Force method (CoGEF) only requires knowledge of the reactants [16]. The CoGEF method allows to investigate the mechanochemical strength of covalent bonds by density functional theory and, recently, it was validated as a predictive tool for mechanochemical reactivity [17]. While multidimensional approaches are also available [18], the classical 1D-CoGEF method is a prominent approach to study mechanochemical reactions due to its simplicity and broad availability. Indeed, similar approaches were already utilized to study the molecular response to external forces before the name CoGEF [16] was suggested by Beyer in 2000 [14].

While investigating the mechanochemical response of epoxy resins with the CoGEF method, we observed that the CoGEF prediction can strongly depend on the initial conformation and the density functional used. Therefore, in this contribution we present an evaluation of the functional dependence of the CoGEF method covering a broad spectrum of different mechanochemical reactivities and force ranges. The results indicate that multiple reactions or reaction cascades can become accessible at the high energetic regions typically observed in 1D-CoGEF calculations. Nevertheless, general relative trends of the mechanochemically interesting descriptors remain mostly independent on the

* Corresponding authors.
E-mail addresses: christian.wick@fau.de (C.R. Wick), ana-suncana.smith@fau.de (A.-S. Smith).

https://doi.org/10.1016/j.finmec.2022.100143
Received 2 August 2022; Received in revised form 2 November 2022; Accepted 2 November 2022
Available online 8 November 2022

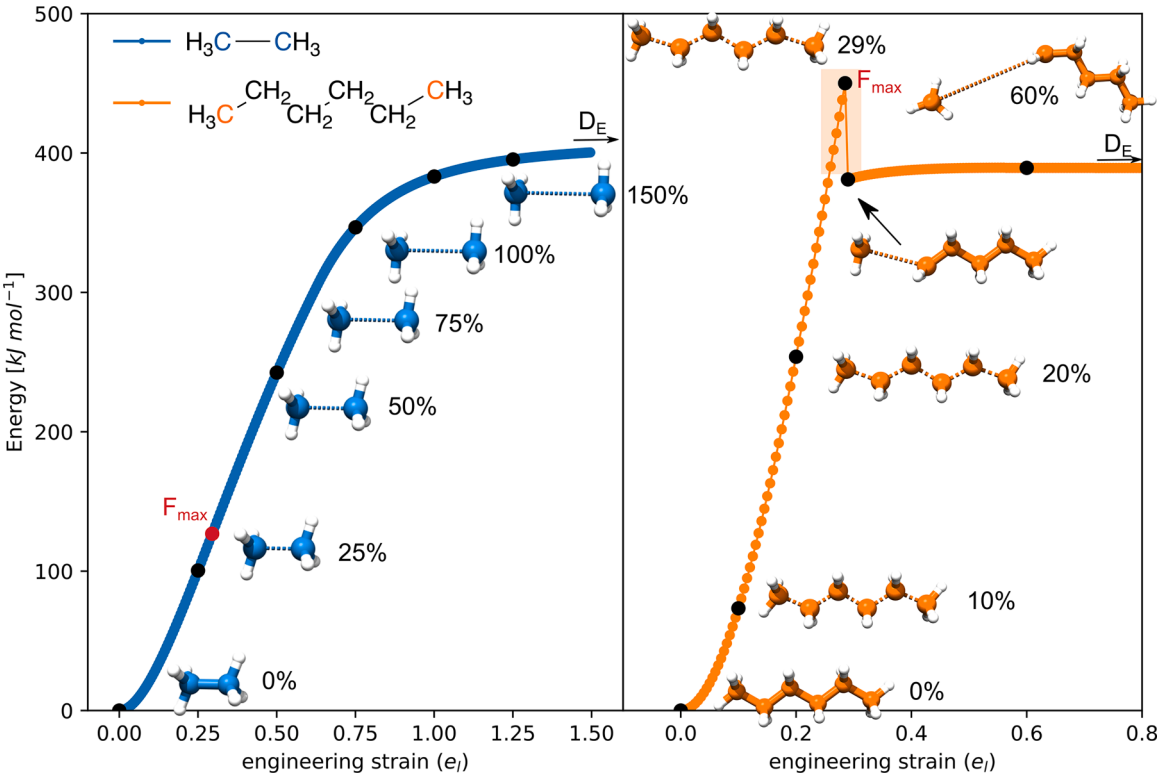

Fig. 1. Bond potential energy surface (BPES) vs. 1-dimensional molecular potential energy surface (1D-MPES). Left: BPES of ethane, Right: 1D-MPES of n-hexane. The point of maximum Force ($F_{max} = \Delta E/\Delta x$) is marked in red, where ΔE is the energetic difference observed for stretching the molecule by Δx. Representative structures along the respective PES are shown next to the graph. In both cases, a relaxed potential energy scan was performed, fixing the distance between the outermost carbon atoms (marked in blue and orange in the chemical structure). Profiles were obtained at the UB3LYP/6-31G(d,p) level of theory.

functional used.

The 1-D CoGEF method

The fundamental assumption underlying the CoGEF approach is that an external force will lead to a distortion of the molecular structure relative to its equilibrium geometry [15]. Consequently, if one imposes the deformation by application of geometrical constraints, one can calculate the force leading to this deformation via the energy change necessary to generate this new geometry. In the 1D-CoGEF approach, a relaxed potential energy scan is performed, incrementally increasing the distance between two atoms to simulate pulling apart of those atoms by an external force. The simplest example of such an approach is a well-known relaxed potential energy scan (PES) of a bond coordinate (Fig. 1). In this example, the bond distance between the two blue carbon atoms is gradually increased and kept constrained, while all other coordinates of the molecule are fully relaxed. This results in a minimum energy profile of the covalent bond as a function of the interatomic distance. We term this energy profile a bond potential energy surface (BPES).

The CoGEF procedure extends this concept to study the behavior of full molecules and not just single bonds as a response to an elongation (simulating the impact of an external force in the direction of the stretching coordinate). For n-hexane for example, a relaxed potential energy scan can be performed while gradually increasing and constraining the distance between the outermost (orange) carbon atoms. With this approach, a molecular potential energy surface (MPES) is obtained which reflects the response of the molecule to an external force acting along the direction of the fixed distance. 1D-CoGEF profiles for more complicated systems, such as n-hexane, typically reveal a discontinuity in the MPES after bond rupture (in the case of n-hexane after 29% strain). The point of maximum Force (F_{max}) can be obtained numerically and is typically located close to the discontinuity before a mechanochemical reaction is observed in an isometric MPES. F_{max} of a BPES is located at the inflection point of the curve. While the BPES approaches the dissociation energy (D_E) at infinite separation, which pinpoints the point of highest energy on the profile, the MPES can contain a high energy region, which is several 100 kJ/mol above the energy at infinite separation after mechanochemical scission. This point of maximum energy is typically denoted as E_{max}. While F_{max} was suggested as a robust predictor of mechanochemical activity in a sense that it can clearly separate mechanochemically active compounds from mechanochemically inactive controls, E_{max} and other predictors such as the force-bond angle prior to bond rupture did not show such a behavior [17]. Although, F_{max} values obtained by 1D-CoGEFF calculations are consistently larger than experimental rupture forces [16,17]. One problem of the 1D-CoGEF method is that it does not explicitly capture the transition states associated with the mechanochemical reactions it aims to predict [18,19]. Therefore, the 1D-CoGEF procedure is not able to compare multiple different mechanochemically induced reactions a single molecule might encounter and the corresponding structure at E_{max} does not necessarily correspond to the proper transition state for the underlying reaction [18]. Two dimensional CoGEF or alternative approaches, which incorporate the external force explicitly, are necessary to fully capture the force transformed energy landscape of mechanochemically activated processes [12,14,18,20]. The predictive character of the 1D-CoGEF method was, however, validated by comparing the scission products obtained after the molecule passes the discontinuity at E_{max} to experimental observations, which indeed showed astonishing agreement at the RB3LYP/6-31G(d) level of theory [17].

Nevertheless, the examples above present very simplified systems and typical polymer models or mechanophores of interest are of much

Covalent polymer backbones

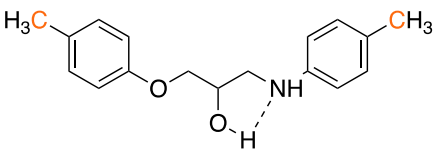

1a

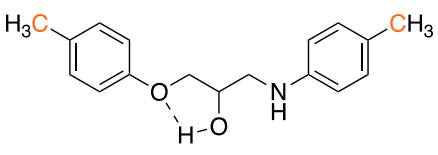

1b

(Epoxy resin)

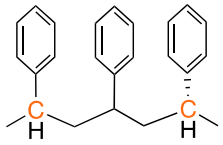

2

(polystyrene)

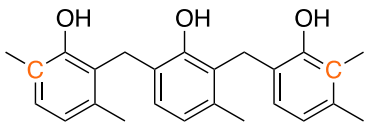

3

(novolak)

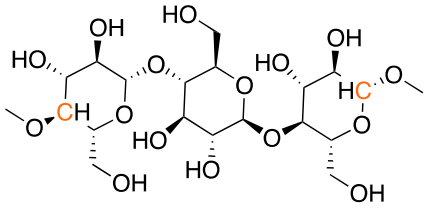

4

(cellulose)

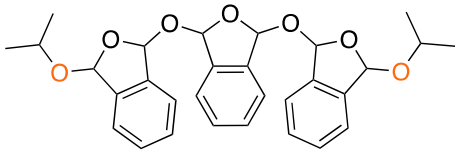

5

(oligo-phthalaldehyde)

Covalent mechanophores

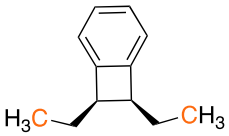

6

(electrocyclic)

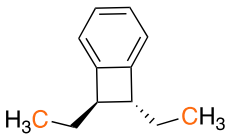

7

(electrocyclic)

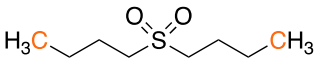

9

(homolytic)

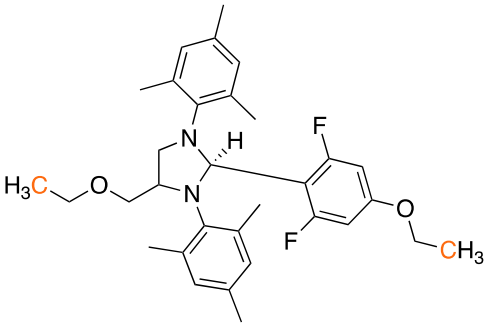

8

(heterolytic)

Non-covalent backbones

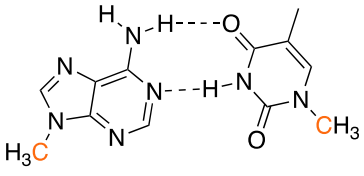

10

(adenine) (thymine)

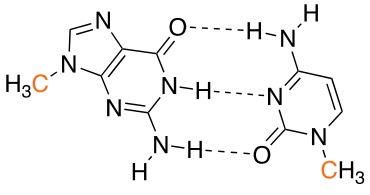

11

(guanine) (cytosine)

Chart 1. Overview of the investigated systems. The constrained atoms are highlighted in orange.

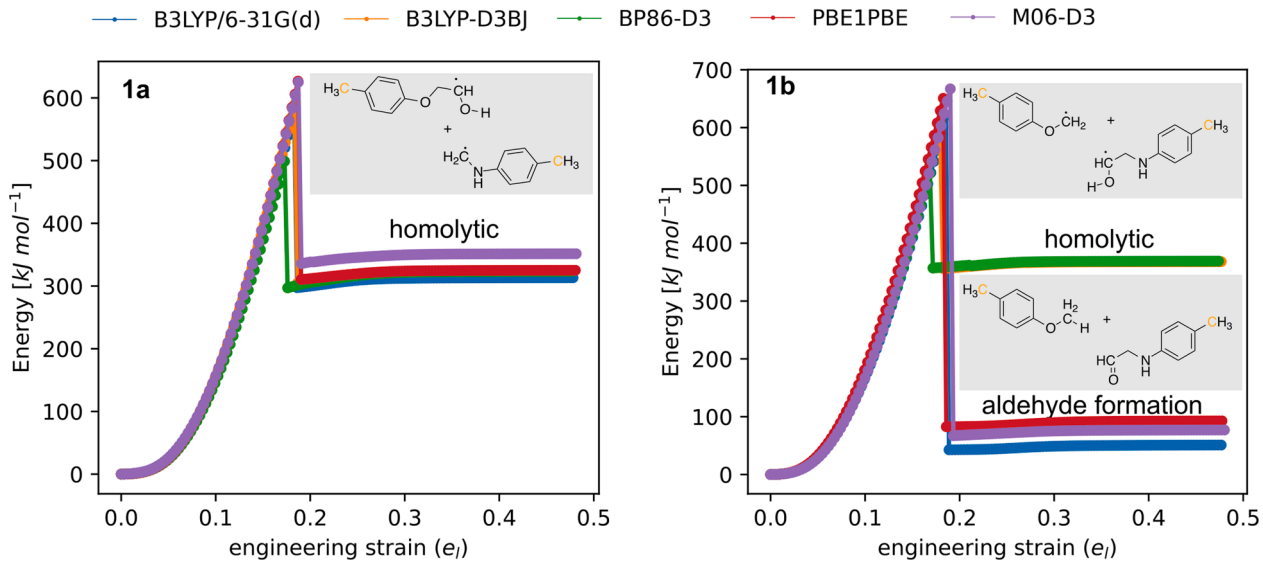

Fig. 2. MPES obtained by means of CoGEF calculations for an epoxy model system in two different conformations (**1a** and **1b**).

higher complexity. In the next sections we will apply the 1D-CoGEF method to a broad range of model compounds covering heterolytic and homolytic bond scission reactions, formal electrocyclic reactions and non-covalent interactions and evaluate the differences between 5 different density functionals (with or without dispersion corrections [21, 22]), namely B3LYP-D3BJ [23–25], M06-D3 [26], PBE1PBE [27] and BP86-D3 [23,28] in combination with the def2-SVP [29] basis set, as well as B3LYP/6-31G(d) [30–32], which developed as the de facto standard in other CoGEF studies. All calculations were performed with Gaussian 16 [33] and the python toolset cogef.py [34] that allows a more advanced procedure including stability analysis and re-optimizations in case an instability was observed in restricted or unrestricted calculations (cf. Fig. S1 and computational details section in the supporting information). The CoGEF increments were set to 0.05 Å, which is in line with previous studies [17] and provided a compromise between accuracy and computational demand (see Table S1 for a comparison of the effect of the step size for n-hexane). The dataset associated with this publication is freely available at Zenodo [35].

Covalent polymer backbones

Chart 1 summarizes all compounds investigated in this study. We will start our discussion with the model compounds representing covalent polymer backbones. Initially, we investigated a model compound of a typical epoxy resin (e.g. consisting of diglycidyl ether of bisphenol A and cured by an amine) in two conformations **1a** and **1b**. This compound presents a typical reaction product after cross-linking of an epoxy group with an amine during the curing phase of thermosetting epoxy resins. The amount of such covalent cross-links determines the molecular material characteristics of the final network structure [36]. The only difference between the two conformations is the presence of hydrogen bonds, which can be formed either between the alcohol group and the amine (1a) or between the alcohol group, the aromatic ether (as acceptor) and the amine as donor (1b). The latter conformation is slightly more stable by only 13 kJ/mol (including zero-point corrections at the B3LYP/6-31G(d) level of theory). The CoGEF profiles for **1a** and **1b** observed with different functionals are summarized in Fig. 2. Please note that the hydrogen bonds were not constrained during the CoGEF calculations, and we did not observe interconversion between the conformers in each run (Fig. S2). The CoGEF calculations, however, reveal different "scission" products. While in **1a** we observe exclusively homolytic bond cleavage (as expected for thermosetting polymers [37–40]) of the carbon-carbon bond between the alcohol and the amine moiety (Fig. 2), a different bond is involved in the mechanochemical scission of the compound in **1b**. Indeed, in this case, the final products that are predicted by the CoGEF calculations depend on the functional used. In two cases, we observe homolytic cleavage of the carbon-carbon bond between the ether and the alcohol (B3LYP-D3BJ, BP86-D3) in three other cases we observe formation of an aldehyde in one step (B3LYP/6-31G(d), PBE1PBE, M06-D3). This result showcases two findings: first, the outcome of the CoGEF calculation depends on the initial conformation and the weakest bond in the system can vary due to local effects (in this case the hydrogen bond is destabilizing the "protected" bond). Second, different functionals not only predict different bond strengths (as previously observed for small molecules [41]) but also completely different mechanochemical scission products.

To investigate such discrepancies further, we conducted CoGEF calculations for the four model polymers **2 – 5** representing typical substructures as observed in polystyrene, novolaks, cellulose or in polyphthalaldehyde (Fig. 3). In the case of our polystyrene model **2**, we observed homolytic bond scission between the outermost ethylbenzene unit and the core backbone. Please note that multiple trials with methyl, propyl or phenyl capping groups attached to both sides of the polystyrene chain always led to cleavage of or reactions with the anchor units instead of the backbone between the repeat units. BP86-D3 predicts rearrangement after radical formation. This directly reflects experimental evidence that homolytic bond scission is predominant [42], however, the radicals generated are short lived and can recombine [10]. Of course, in a more realistic larger polymer model the radical reactions after bond cleavage would not be limited to this interaction but could easily show a large diversity.

While we observed homolytic bond cleavage leading to identical scission products for the polystyrene model **3** in all five cases, the cellulose trimer **4** and the oligophthalaldehyde **5** again show a functional dependence. CoGEF predicts either homolytic scission of a glycosidic bond (B3LYP, BP86-D3, PBE1PBE) in **4**, or fragmentation with release of

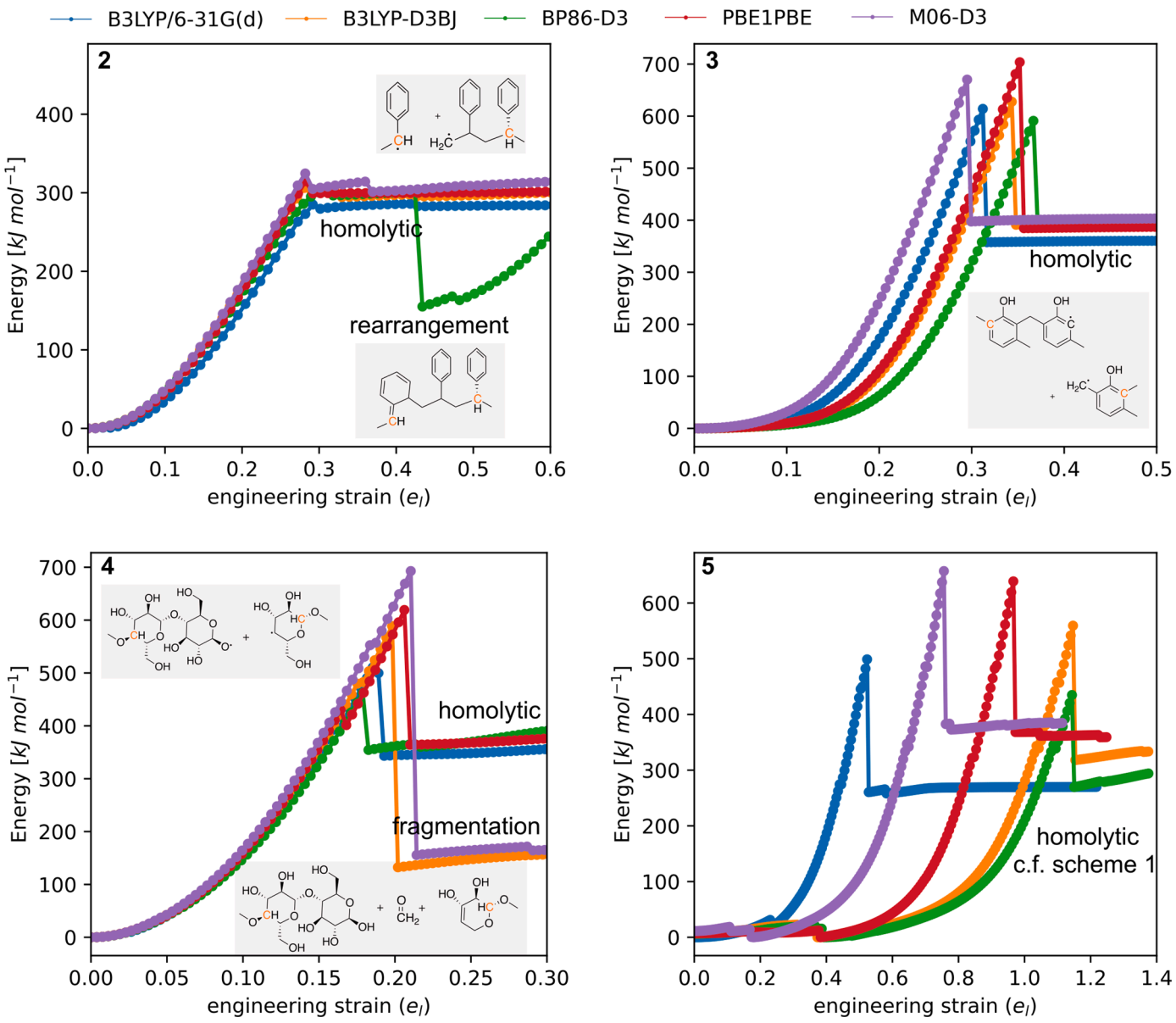

Fig. 3. MPES obtained by means of CoGEF calculations for covalent polymer backbones represented by compounds **2, 3, 4** and **5**. The different scission products are shown as insets. For compound **5**, the unrestricted MPES is shown, which in all cases predicts homolytic bond scission. The restricted MPES (which would indicate heterolytic bond scission) suffer an RKS/UKS instability and converge to the unrestricted profiles (cf. Figure S03). The scission products for compound **5** can be found in Scheme 1.

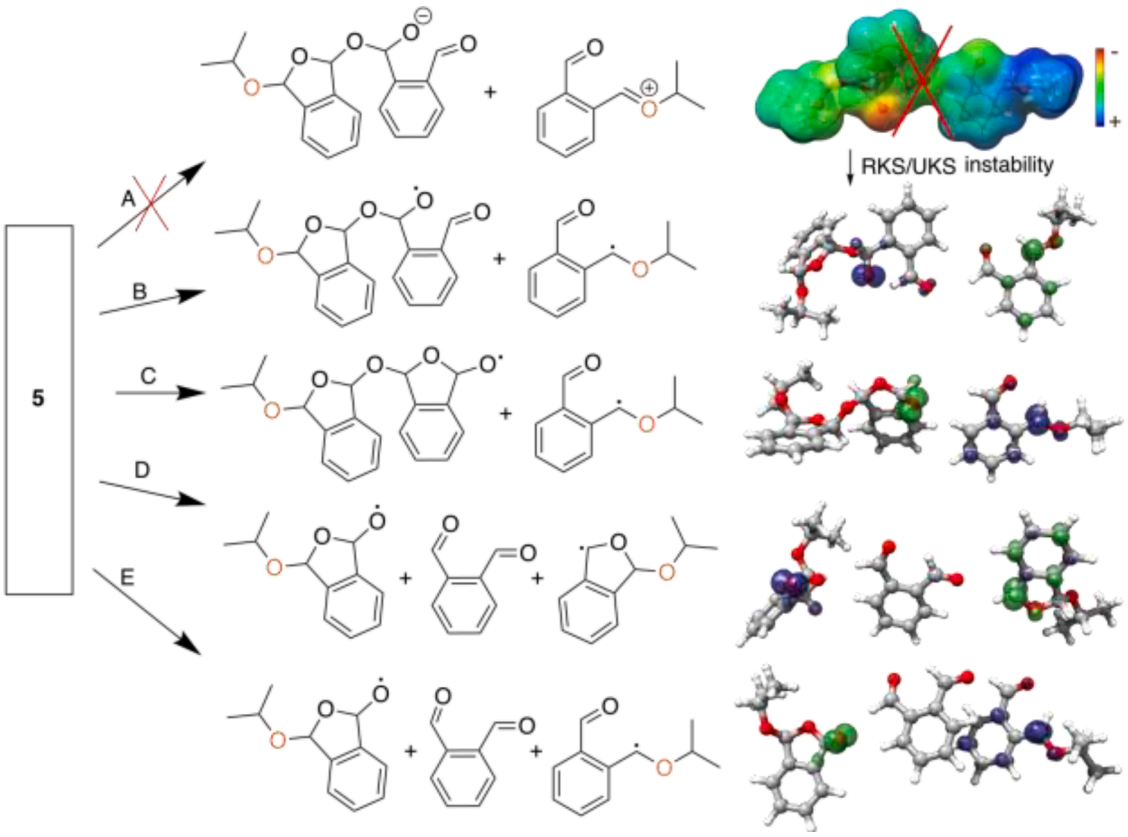

Scheme 1. Different mechanochemical scission products predicted by the CoGEF procedure for Poly(phthalaldehyde) **5** with different functionals. The electrostatic potential is shown for the anticipated heterolytic scission product for path A. However, all scission products observed with the restricted CoGEF procedure suffer a severe RKS / UKS instability and the stable wavefunctions clearly indicate homolytic bond scission in all cases. The spin density (computed for the stable UKS wavefunctions) is shown for the paths B, C, D and E in the right column.

formaldehyde (B3LYP-D3BJ, M06-D3). Again, this happens in one step without homolytic intermediates. The scission products differ by roughly 200 kJ mol^{-1} in energy and the rupture happens after E_{max} of 460-690 kJ mol^{-1} is reached. It seems to be likely that multiple barriers vanish at this high energy region on the MPES, and it is not surprising that the predicted scission products show a functional dependence. This behavior is even more pronounced in the case of the oligophthalaldehyde **5**. In previous combined experimental and theoretical studies, oligophthalaldehydes were shown to follow a heterolytic unzipping pathway by using a combination of sophisticated trapping experiments and steered molecular dynamics simulations [43]. The steered molecular dynamics approach was conducted with unrestricted density functional theory at the B3LYP/6-31G and B3LYP/6-31G(d,f) levels of theory and indicated that an initial heterolytic depolymerization is indeed followed by radical formation (indicated by an immediate rise of the expectation value of the spin squared operator <S2> to ~1.0) [43]. Interestingly, previous 1D-CoGEF calculations conducted at the restricted B3LYP/6-31G(d) level of theory predicted only heterolytic scission products [17]. Our CoGEF calculations on compound **5**, however, do not confirm the heterolytic bond scission. A close inspection of the wavefunctions instead confirmed a plethora of different homolytic scission products (Scheme 1), all of which support the idea of a radical unzipping pathway. The discrepancies between previous studies and our results are therefore most likely attributable to the usage of restricted wavefunctions, which prohibit the identification of homolytic scission products. While restricted (RKS) and unrestricted Kohn-Sham (UKS) approaches are identical up to the rupture event on the MPES, a stability analysis of the scission products obtained with RKS revealed RKS/UKS instabilities with all tested functionals (Fig. S3). The observed maximum Forces are identical between UKS and RKS procedures (Table 2 and Table S1) and are in excellent agreement with previous studies at the B3LYP/6-31G(d) level of theory, which observed a F_{max} equal to 5.6 nN [17]. It is noteworthy that the presented calculations were conducted on an all-cis isomer of **5**, similar to previous work [17]. Additionally, we performed test calculations on an all-trans isomer, which indicate that in this case also a homolytic scission pathway is prevailing (SI), however, the scission products again differ from the ones delineated in Scheme 1.

The observed mechanochemical descriptors are summarized in Table 1. The largest relative standard deviation (RSD) of the maximum Force was observed for compound **5** with 13%. This compares to an overall RSD of F_{max} of 8 % for all covalent polymer backbones investigated. However, it is worth mentioning that the RSD for F_{max} for compounds **1a, 1b** and **3**, is relatively constant around 4.5-6%. This indicates that F_{max} is rather independent on the predicted reaction in these cases. The largest deviation is observed for E_{max}, as expected and relates to an RSD of 11.9 % for all covalent backbones. The observed fracture strain shows an RSD of almost 10 %, which again appears to be rather independent on the predicted reaction.

It is, however, very interesting that even in simple covalent polymeric backbones, i.e. without any mechanophoric component, different (unexpected) mechanochemical reactions besides homolytic bond scission might be observed with the CoGEF procedure. There is no guarantee, that every functional will predict an identical reactivity. In general, the MPES obtained by the CoGEF procedure exerts very high energetic regions before bond rupture. At such high energies, multiple reactions might become accessible so that the result of the CoGEF procedure depends on the functional used.

Table 1
Mechanochemical descriptors obtained from CoGEF calculations for covalent polymer backbones.

System	F_{max} [nN]	E_{max} [kJ/mol]	Strain at F_{max} [%]	Type
1a (epoxy)				
B3LYP/6-31G(d)	6.5	578.8	18.3	homolytic
B3LYP-D3BJ/def2SVP	6.7	588.8	18.3	homolytic
BP86-D3/def2SVP	6.1	498.9	17.3	homolytic
PBE1PBE/def2SVP	7.0	626.8	18.7	homolytic
M06-D3/def2SVP	6.9	625.1	18.7	homolytic
SD	**0.4**	**52.0**	**0.6**	
RSD (%)	**5.5**	**8.9**	**3.2**	
1b (epoxy)				
B3LYP/6-31G(d)	6.7	620.7	18.6	aldehyde form.
B3LYP-D3BJ/def2SVP	6.8	603.7	17.9	homolytic
BP86-D3/def2SVP	6.2	520.8	16.9	homolytic
PBE1PBE/def2SVP	7.1	650.7	18.3	aldehyde form.
M06-D3/def2SVP	7.1	667.0	19.0	aldehyde form.
SD	**0.4**	**57.0**	**0.8**	
RSD (%)	**5.4**	**9.3**	**4.5**	
2 (polystyrene)				
B3LYP/6-31G(d)	5.1	285.1	26.3	homolytic
B3LYP-D3BJ/def2SVP	5.3	306.2	24.2	homolytic
BP86-D3/def2SVP	5.0	303.5	24.1	hom. + rearr.
PBE1PBE/def2SVP	5.7	314.8	27.3	homolytic
M06-D3/def2SVP	5.7	324.6	26.3	homolytic
SD	**0.3**	**14.7**	**1.4**	
RSD	**5.8**	**4.8**	**5.4**	
3 (novolak)				
B3LYP/6-31G(d)	7.0	614.0	31.2	homolytic
B3LYP-D3BJ/def2SVP	7.2	627.7	34.3	homolytic
BP86-D3/def2SVP	6.8	591.0	36.7	homolytic
PBE1PBE/def2SVP	7.6	703.7	35.2	homolytic
M06-D3/def2SVP	7.5	670.2	29.5	homolytic
SD	**0.3**	**45.3**	**2.9**	
RSD	**4.5**	**7.1**	**8.8**	
4 (cellulose)				
B3LYP/6-31G(d)	6.7	510.5	18.5	homolytic
B3LYP-D3BJ/def2SVP	7.2	588.8	19.8	fragmentation
BP86-D3/def2SVP	6.2	462.7	17.9	homolytic
PBE1PBE/def2SVP	7.7	619.2	20.6	homolytic
M06-D3/def2SVP	7.9	692.8	21.0	fragmentation
SD	**0.7**	**90.5**	**1.3**	
RSD (%)	**9.9**	**15.8**	**6.9**	
5 (oligo-phtalaldehyde)				
B3LYP/6-31G(d)	5.5	498.9	52.3	homolytic B
B3LYP-D3BJ/def2SVP	5.9	559.4	56.3	homolytic C
BP86-D3/def2SVP	4.8	434.9	53.9	homolytic C
PBE1PBE/def2SVP	6.5	638.9	42.2	homolytic D
M06-D3/def2SVP	6.7	657.3	48.9	homolytic E
SD	**0.8**	**93.6**	**5.5**	
RSD (%)	**13.0**	**16.8**	**10.8**	
$SD_{polymers}$	**0.5**	**64.8**	**2.7**	
$RSD_{polymers}$ (%)	**8.0**	**11.9**	**9.8**	

Covalent mechanophores

While homolytic bond scission is prevailing in polymeric compounds, mechanophores can exhibit new chemistry, which is only accessible by mechanical force. One well-known example is the mechanically induced electrocyclic ring opening reaction of benzocyclobutene [2,11]. A mechanical force can open the ring in either a trans (**6**) or cis (**7**) fashion as showcased in our model compounds **6** and **7** respectively. It was observed that the cis pathway will follow a disrotatory mechanism, which even violates the Woodward-Hoffmann rules [2]. Therefore, this system is a wonderful example how mechanic force can open pathways to new or otherwise forbidden chemistry. All of our CoGEF calculations on model systems **6** and **7** show the same electrocyclic scission products (Fig. 4). No radical generation is observed along the MPES, indicating that only the electrocyclic mechanism is accessible in these compounds. This is in line with experiments and previous computational studies on this system [2,11,17].

Mechanophore **8** was reported to undergo either heterocyclic ring opening or direct formation of an n-heterocyclic carbene via a concerted pathway [44]. Our CoGEF calculations confirm the heterolytic bond scission for molecule **8** for all functionals, which is in line with previous CoGEF calculations [17]. Neither a radical pathway nor a scission product following a concerted pathway was observed and all restricted wavefunctions were indeed stable minima, in contrast to our observations for the oligo-phthalaldehyde **5**. BP86-D3 predicts that a proton can be easily abstracted by the anionic scission partner, which is corroborated by experiments [44]. It is, however, not the proton located at the heterocycle that is abstracted. Instead, a methyl proton is abstracted followed by ring closure as depicted in Fig. 4. The last mechanophore investigated is the sulfone **9** (which indeed could also be categorized as a covalent polymer backbone). In this case all functionals indicate identical homolytic scission products. The deviation between the results with different functionals for the covalent mechanophores follow the trends observed for the covalent polymeric backbones (Table 2). The largest differences are again observed for E_{max} with an RSD of 11 %.

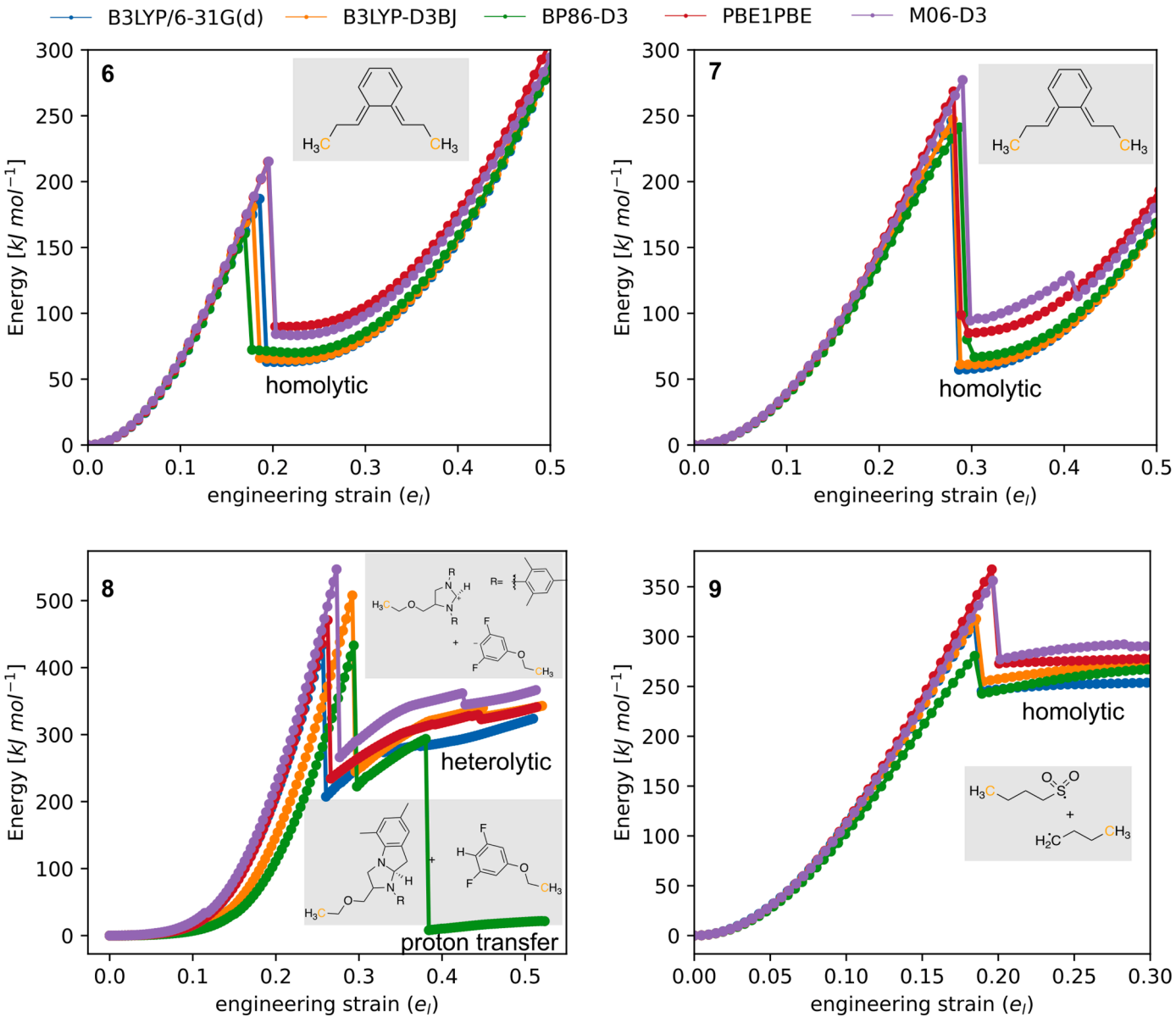

Fig. 4. MPES obtained by means of CoGEF calculations for different covalent mechanophores.

Table 2
Mechanochemical descriptors obtained from CoGEF calculations for different mechanophores.

System	F_{max} [nN]	E_{max} [kJ/mol]	Strain at F_{max} [%]	Type
6				
B3LYP/6-31G(d)	4.1	186.9	17.8	4π electrocyclic
B3LYP-D3BJ/def2SVP	4.2	180.9	17.0	4π electrocyclic
BP86-D3/def2SVP	3.9	160.5	16.2	4π electrocyclic
PBE1PBE/def2SVP	4.5	215.0	18.7	4π electrocyclic
M06-D3/def2SVP	4.5	215.3	18.0	4π electrocyclic
SD	**0.3**	**23.5**	**0.9**	
RSD (%)	**6.5**	**12.3**	**5.4**	
7				
B3LYP/6-31G(d)	3.7	246.0	24.5	4π electrocyclic
B3LYP-D3BJ/def2SVP	3.7	247.2	22.2	4π electrocyclic
BP86-D3/def2SVP	3.4	241.2	23.8	4π electrocyclic
PBE1PBE/def2SVP	4.2	268.5	25.6	4π electrocyclic
M06-D3/def2SVP	4.1	277.2	25.7	4π electrocyclic
SD	**0.3**	**15.8**	**1.4**	
RSD (%)	**8.6**	**6.2**	**5.9**	
8				
B3LYP/6-31G(d)	5.5	434.2	25.7	heterolytic
B3LYP-D3BJ/def2SVP	5.9	507.8	29.2	heterolytic
BP86-D3/def2SVP	5.4	433.1	29.4	heterolytic
PBE1PBE/def2SVP	5.9	470.9	26.2	heterolytic
M06-D3/def2SVP	6.2	546.7	27.3	heterolytic
SD	**0.3**	**49.0**	**1.7**	
RSD (%)	**6.0**	**10.2**	**6.1**	
9				
B3LYP/6-31G(d)	4.0	314.4	16.1	homolytic
B3LYP-D3BJ/def2SVP	4.1	317.7	16.2	homolytic
BP86-D3/def2SVP	3.5	280.7	14.7	homolytic
PBE1PBE/def2SVP	4.5	367.4	17.2	homolytic
M06-D3/def2SVP	4.3	356.1	17.3	homolytic
SD	**0.4**	**34.9**	**1.1**	
RSD (%)	**9.2**	**10.7**	**6.5**	
$SD_{mech.}$	**0.3**	**33.2**	**1.3**	
$RSD_{mech.}$	**7.5**	**10.6**	**6.1**	

Non-covalent backbones

The last class of compounds in this study are non-covalent backbones. We chose two very prominent examples, namely the hydrogen bonding complexes between the DNA base-pairs adenine and thymine 10, and guanine and cytosine 11. Applying the CoGEF procedure on those complexes leads to the observed MPES shown in Fig. 5. In those MPESs, no discontinuity is observed and the overall behavior resembles more that of a classical BPES. Looking at the Force over strain plots in the lower part of Fig. 5, one can easily deduce two maxima associated with two consecutive rupture events in those complexes. Indeed, in case of 11 two hydrogen bonds are lost after 9.5% strain and the last one persists up to 38 % strain. The maximum Force observed for those hydrogen bonds is 1 order of magnitude smaller then for covalent bonds, as expected. While the absolute values of the SDs of the descriptors shown in Table 3 are therefore also significantly smaller than those observed for the covalently bonded compounds, the RSDs are the highest among the investigated systems. All F_{max} values have RSDs close to or exceeding the 10 % mark and the overall RSD for all systems is the largest (above 12 %). It was repeatedly reported that the maximum Force predicted by CoGEF calculations is far from the values observed experimentally. One possible reason for this is the neglect of temperature effects [15,17]. This observation is also true for the hydrogen bonded base-pairs studied in this work. The experimentally determined force to unzip guanine-cytosine was reported to be 20 ± 3 pN, whereas the force to unbind adenine-thymine pairs is 9 ± 3 pN [45]. This is again one order of magnitude smaller than predicted by the CoGEF methods, independent on the functional used.

In the case of non-covalent interaction compounds, of course no mechanochemical reaction will be observed since the non-covalent interactions are the weakest points in the system. The huge energetic differences observed with different functionals however emphasize that one should expect large differences in CoGEF calculations on complicated systems, which contain multiple non-covalent as well as covalent interactions along the direction of the external force.

Conclusions

In this work we investigated the impact the choice of density functional can have on the outcome and prediction of CoGEF calculations across a broad set of molecules and reaction types. This includes homolytic, heterolytic, mechanochemically induced (forbidden) reactions and the disruption of non-covalent interactions. Most importantly, we found that, in amine-cured aromatic epoxy resins, multiple bonds have similar mechanic strength and homolytic bond breakage depends on the local structure and conformation of the resin moieties. Even direct formation of aldehydes might be observed, but only for a subset of density functionals. Furthermore, our CoGEF calculations on the unzipping reaction of polyphthalaldehyde indicate that a radical mechanism prevails over the heterolytic one, since the computed RKS wavefunctions indicate RKS/UKS instabilities that lead to thermodynamically more favorable homolytic scission products. Nevertheless, this behavior might change in other media than the gas phase.

In terms of the robustness of typical CoGEF descriptors, we observed the greatest functional dependence for E_{max} in our CoGEF calculations. The relative deviation for F_{max} is, in general, smaller than for E_{max}, however one should expect differences up to at least 17 %. We summarized all predicted maximum forces for all model systems again in Fig. 6. It is evident that the maximum forces to break polymer chains and activate mechanophores are overlapping. In other words, there is no clear fundamental separation between the ranges of maximum force to break a covalent polymer backbone or a covalent mechanophore. This means that there might be competing reactions depending on the polymer system and mechanophores used in novel mechanoactive polymeric materials. Non-covalent bonds can only withstand forces of at least one order of magnitude smaller than typical covalent bonds, based on the CoGEF calculations, which is an expected result. Nevertheless, while the spread of maximum forces observed for different functionals shows large deviations, the relative trend (i.e. the vertical ordering of the functionals in Fig. 6) is consistent and the qualitative trends of the bond strengths are preserved among the functionals for covalent mechanophores or backbones. Unfortunately, this is independent of the actual scission products predicted by the CoGEF method and different functionals can predict completely different reactivity patterns. The

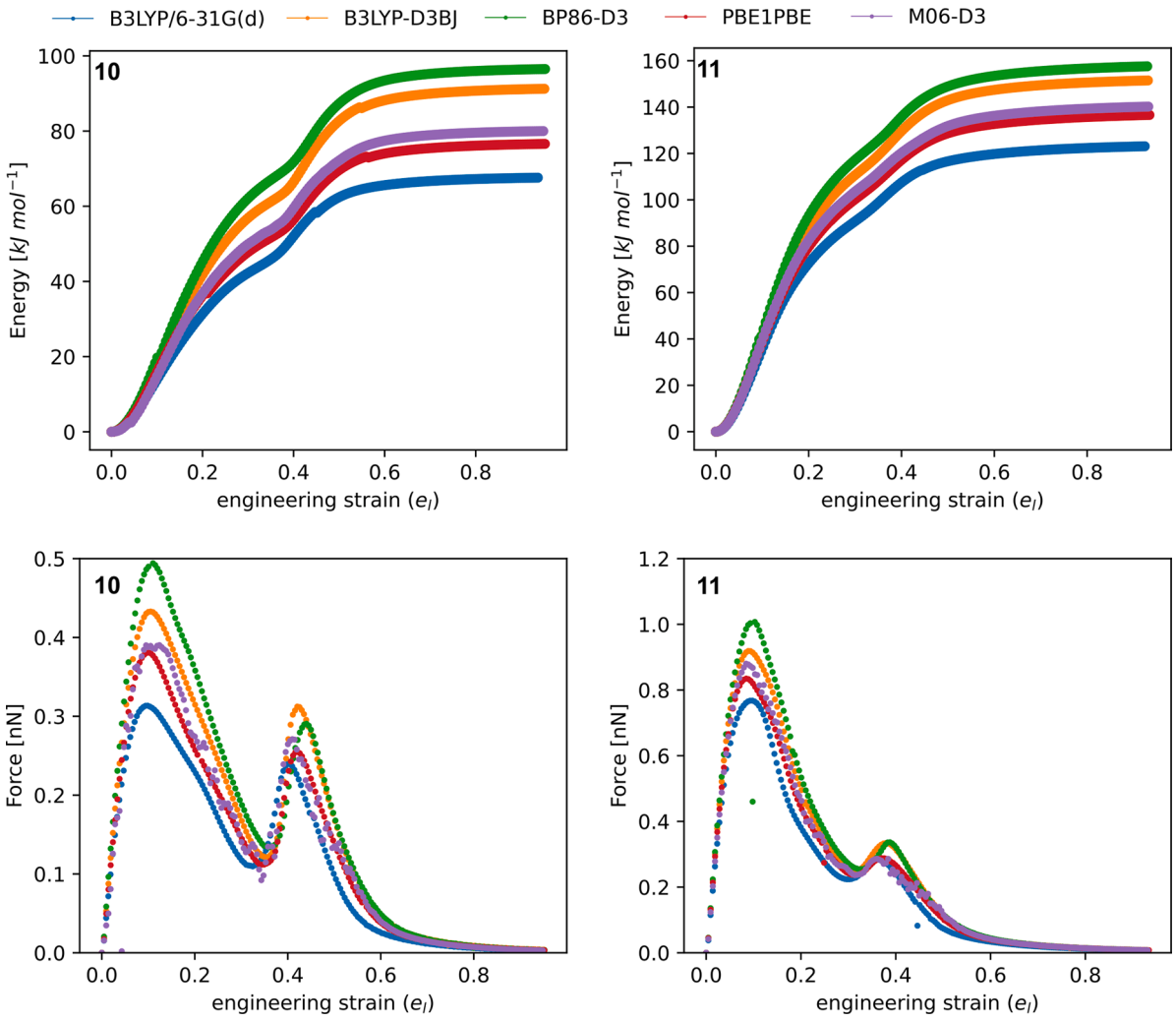

Fig. 5. MPES and resulting forces obtained by means of CoGEF calculations for non-covalent backbone models **10** and **11**. Top: MPES profiles up to 100% strain. Bottom corresponding force profiles. The two maxima indicate the rupture of the hydrogen bonds present in the system.

Table 3
Mechanochemical descriptors obtained from CoGEF calculations for non-covalent backbone model systems.

System	F_{max} [nN]	E_{max} [kJ/mol]	Strain at F_{max} [%]	Type
10 HB1				
B3LYP/6-31G(d)	0.31	-	9.9	HB-1
B3LYP-D3BJ/def2SVP	0.43	-	10.5	HB-1
BP86-D3/def2SVP	0.49	-	11.0	HB-1
PBE1PBE/def2SVP	0.38	-	10.0	HB-1
M06-D3/def2SVP	0.39	-	12.4	HB-1
SD	**0.07**	**-**	**1.0**	
RSD (%)	**16.6**	**-**	**9.4**	
10 HB2				
B3LYP/6-31G(d)	0.24	67.6	40.0	HB-2
B3LYP-D3BJ/def2SVP	0.31	91.2	42.5	HB-2
BP86-D3/def2SVP	0.29	96.5	44.0	HB-2
PBE1PBE/def2SVP	0.25	76.6	42.1	HB-2
M06-D3/def2SVP	0.27	80.0	41.0	HB-2
SD	**0.03**	**11.6**	**1.5**	
RSD (%)	**10.4**	**14.0**	**3.7**	
11 HB1+2				
B3LYP/6-31G(d)	0.77	-	9.8	HB-1 + HB-2
B3LYP-D3BJ/def2SVP	0.92	-	8.9	HB-1 + HB-2
BP86-D3/def2SVP	1.01	-	10.3	HB-1 + HB-2
PBE1PBE/def2SVP	0.83	-	8.4	HB-1 + HB-2
M06-D3/def2SVP	0.88	-	8.4	HB-1 + HB-2
SD	**0.09**	**-**	**0.8**	
RSD (%)	**10.2**	**-**	**9.0**	
11 HB3				
B3LYP/6-31G(d)	0.28	123.1	36.2	HB-3
B3LYP-D3BJ/def2SVP	0.33	151.5	37.9	HB-3
BP86-D3/def2SVP	0.34	157.6	38.8	HB-3
PBE1PBE/def2SVP	0.29	136.6	37.1	HB-3
M06-D3/def2SVP	0.29	140.2	36.0	HB-3
SD	**0.03**	**13.4**	**1.1**	
RSD (%)	**8.9**	**9.5**	**3.1**	
$SD_{non-cov.}$	**0.06**	**12.5**	**1.2**	
$RSD_{non-cov.}$ (%)	**12.8**	**11.2**	**4.7**	

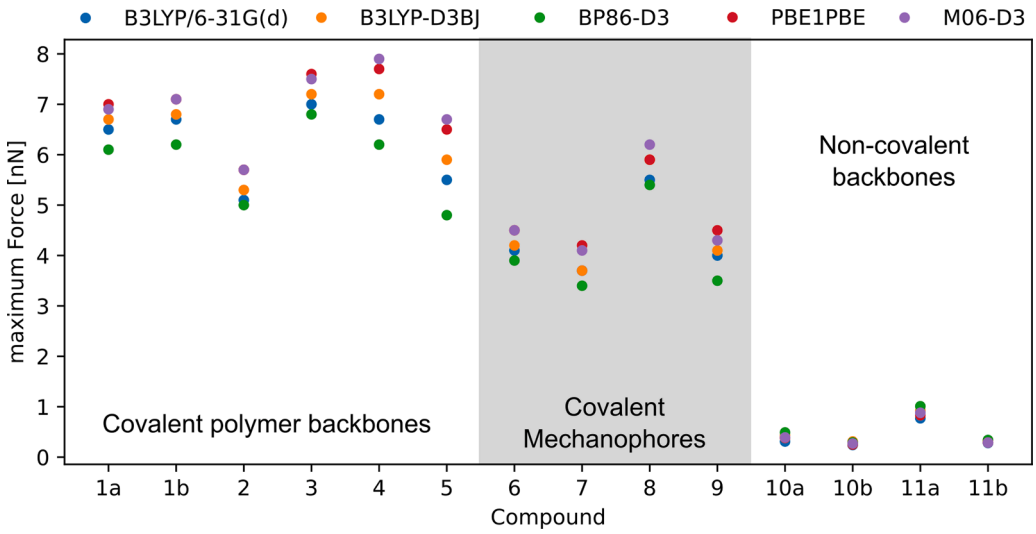

Fig. 6. Summary of maximum Forces obtained by CoGEF calculations.

presence of additional non-covalent interactions can, in addition, directly influence the outcome of the CoGEF calculations and lead to different scission products as was observed for epoxies **1a** and **1b**. It is, therefore, of high importance to validate the 1D-CoGEF predictions against additional experimental data and to cross check the observations with other computational approaches that can compare different mechanochemically induced transition states to truly confirm the observed reactivity.

Funding Sources

This research was funded by the Deutsche Forschungsgemeinschaft (DFG, German Research Foundation) - 377472739/GRK 2423/1-2019 FRASCAL. The authors are very grateful for this support.

CRediT authorship contribution statement

Christian R. Wick: Conceptualization, Data curation, Formal analysis, Investigation, Methodology, Software, Validation, Visualization, Writing – original draft, Writing – review & editing. **Ece Topraksal:** Formal analysis, Validation, Visualization. **David M. Smith:** Conceptualization, Supervision, Validation, Writing – review & editing. **Ana-Sunčana Smith:** Conceptualization, Funding acquisition, Supervision, Validation, Writing – review & editing.

Declaration of Competing Interest

There are no conflicts to declare.

Data Availability

The dataset and the code accompanying this puplication are available at Zenodo: doi.org/10.5281/zenodo.7215554 and doi.org/10.5281/zenodo.7079733.

Acknowledgment

This research was funded by the Deutsche Forschungsgemeinschaft (DFG, German Research Foundation) - 377472739/GRK 2423/1-2019 FRASCAL. The authors are very grateful for this support.

Supplementary materials

Supplementary material associated with this article can be found, in the online version, at doi:10.1016/j.finmec.2022.100143.

References

[1] J.J. Gilman, Mechanochemistry, Science 274 (1996), https://doi.org/10.1126/science.274.5284.65, 65–65.
[2] C.R. Hickenboth, J.S. Moore, S.R. White, N.R. Sottos, J. Baudry, S.R. Wilson, Biasing reaction pathways with mechanical force, Nature 446 (2007) 423–427, https://doi.org/10.1038/nature05681.
[3] M.M. Caruso, D.A. Davis, Q. Shen, S.A. Odom, N.R. Sottos, S.R. White, J.S. Moore, Mechanically-induced chemical changes in polymeric materials, Chem. Rev. 109 (2009) 5755–5798, https://doi.org/10.1021/cr9001353.
[4] N. Willis-Fox, E. Rognin, T.A. Aljohani, R. Daly, Polymer mechanochemistry: manufacturing is now a force to be reckoned with, Chem 4 (2018) 2499–2537, https://doi.org/10.1016/j.chempr.2018.08.001.
[5] M.K. Beyer, H. Clausen-Schaumann, Mechanochemistry: the mechanical activation of covalent bonds, Chem. Rev. 105 (2005) 2921–2948, https://doi.org/10.1021/cr030697h.
[6] K.M. Wiggins, J.N. Brantley, C.W. Bielawski, Polymer mechanochemistry: force enabled transformations, ACS Macro Lett 1 (2012) 623–626, https://doi.org/10.1021/mz300167y.
[7] J.L. Howard, Q. Cao, D.L. Browne, Mechanochemistry as an emerging tool for molecular synthesis: what can it offer? Chem. Sci. 9 (2018) 3080–3094, https://doi.org/10.1039/C7SC05371A.
[8] A.L. Black, J.M. Lenhardt, S.L. Craig, From molecular mechanochemistry to stress-responsive materials, J. Mater. Chem. 21 (2011) 1655–1663, https://doi.org/10.1039/C0JM02636K.
[9] H. Hu, Z. Ma, X. Jia, Reaction cascades in polymer mechanochemistry, Mater. Chem. Front. 4 (2020) 3115–3129, https://doi.org/10.1039/D0QM00435A.
[10] S. Akbulatov, R. Boulatov, Experimental polymer mechanochemistry and its interpretational frameworks, ChemPhysChem 18 (2017) 1422–1450, https://doi.org/10.1002/cphc.201601354.
[11] M.T. Ong, J. Leiding, H. Tao, A.M. Virshup, T.J. Martínez, First principles dynamics and minimum energy pathways for mechanochemical ring opening of cyclobutene, J. Am. Chem. Soc. 131 (2009) 6377–6379, https://doi.org/10.1021/ja8095834.
[12] J. Ribas-Arino, M. Shiga, D. Marx, Understanding covalent mechanochemistry, Angew. Chem. Int. Ed. 48 (2009) 4190–4193, https://doi.org/10.1002/anie.200900673.
[13] A.G. Roessler, P.M. Zimmerman, Examining the ways to bend and break reaction pathways using mechanochemistry, J. Phys. Chem. C. 122 (2018) 6996–7004, https://doi.org/10.1021/acs.jpcc.8b00467.
[14] J. Ribas-Arino, D. Marx, Covalent mechanochemistry: theoretical concepts and computational tools with applications to molecular nanomechanics, Chem. Rev. 112 (2012) 5412–5487, https://doi.org/10.1021/cr200399q.
[15] T. Stauch, A. Dreuw, Advances in quantum mechanochemistry: electronic structure methods and force analysis, Chem Rev. (2016) 44, https://doi.org/10.1021/acs.chemrev.6b00458.
[16] M.K. Beyer, The mechanical strength of a covalent bond calculated by density functional theory, J. Chem. Phys. 112 (2000) 7307–7312, https://doi.org/10.1063/1.481330.
[17] I.M. Klein, C.C. Husic, D.P. Kovács, N.J. Choquette, M.J. Robb, Validation of the CoGEF method as a predictive tool for polymer mechanochemistry, J. Am. Chem. Soc. 142 (2020) 16364–16381, https://doi.org/10.1021/jacs.0c06868.
[18] O. Brügner, M. Walter, Temperature and loading rate dependent rupture forces from universal paths in mechanochemistry, Phys. Rev. Mater. 2 (2018), 113603, https://doi.org/10.1103/PhysRevMaterials.2.113603.
[19] S.M. Avdoshenko, D.E. Makarov, Reaction coordinates and pathways of mechanochemical transformations, J. Phys. Chem. B. 120 (2016) 1537–1545, https://doi.org/10.1021/acs.jpcb.5b07613.
[20] T.J. Kucharski, R. Boulatov, The physical chemistry of mechanoresponsive polymers, J. Mater. Chem. 21 (2011) 8237, https://doi.org/10.1039/c0jm04079g.
[21] S. Grimme, S. Ehrlich, L. Goerigk, Effect of the damping function in dispersion corrected density functional theory, J. Comput. Chem. 32 (2011) 1456–1465, https://doi.org/10.1002/jcc.21759.
[22] S. Grimme, J. Antony, S. Ehrlich, H. Krieg, A consistent and accurate *ab initio* parametrization of density functional dispersion correction (DFT-D) for the 94 elements H-Pu, J. Chem. Phys. 132 (2010), 154104, https://doi.org/10.1063/1.3382344.
[23] A.D. Becke, Density-functional exchange-energy approximation with correct asymptotic behavior, Phys Rev A 38 (1988) 3098–3100, https://doi.org/10.1103/physreva.38.3098.
[24] C. Lee, W. Yang, R.G. Parr, Development of the Colle-Salvetti correlation-energy formula into a functional of the electron density, Phys Rev B 37 (1988) 785–789, https://doi.org/10.1103/PhysRevB.37.785.
[25] B. Miehlich, A. Savin, H. Stoll, H. Preuss, Results obtained with the correlation energy density functionals of becke and Lee, Yang and Parr, Chem. Phys. Lett. 157 (1989) 200–206, https://doi.org/10.1016/0009-2614(89)87234-3.
[26] Y. Zhao, D. Truhlar, The M06 suite of density functionals for main group thermochemistry, thermochemical kinetics, noncovalent interactions, excited states, and transition elements: two new functionals and systematic testing of four M06-class functionals and 12 other functionals, Theor. Chem. Acc. 120 (2008) 215–241, https://doi.org/10.1007/s00214-007-0310-x.
[27] C. Adamo, V. Barone, Toward reliable density functional methods without adjustable parameters: the PBE0 model, J. Chem. Phys. 110 (1999) 6158–6170, https://doi.org/10.1063/1.478522.
[28] J.P. Perdew, Density-functional approximation for the correlation-energy of the inhomogeneous electron-gas, Phys. Rev. B. 33 (1986) 8822–8824, https://doi.org/10.1103/Physrevb.33.8822.
[29] F. Weigend, R. Ahlrichs, Balanced basis sets of split valence, triple zeta valence and quadruple zeta valence quality for H to Rn: Design and assessment of accuracy, Phys. Chem. Chem. Phys. 7 (2005) 3297–3305, https://doi.org/10.1039/B508541A.
[30] R. Ditchfield, W.J. Hehre, J.A. Pople, Self-consistent molecular-orbital methods. IX. An extended gaussian-type basis for molecular-orbital studies of organic molecules, J. Chem. Phys. 54 (1971) 724–728, https://doi.org/10.1063/1.1674902.
[31] W.J. Hehre, R. Ditchfield, J.A. Pople, Self-consistent molecular orbital methods. XII. Further extensions of gaussian-type basis sets for use in molecular orbital studies of organic molecules, J. Chem. Phys. 56 (1972) 2257–2261, https://doi.org/10.1063/1.1677527.
[32] P.C. Hariharan, J.A. Pople, The influence of polarization functions on molecular orbital hydrogenation energies, Theor. Chem. Acc. 28 (1973) 213–222, https://doi.org/10.1007/bf00533485.
[33] M.J. Frisch, G.W. Trucks, H.B. Schlegel, G.E. Scuseria, M.A. Robb, J.R. Cheeseman, G. Scalmani, V. Barone, G.A. Petersson, H. Nakatsuji, X. Li, M. Caricato, A.V. Marenich, J. Bloino, B.G. Janesko, R. Gomperts, B. Mennucci, H.P. Hratchian, J.V. Ortiz, A.F. Izmaylov, J.L. Sonnenberg, Williams, F. Ding, F. Lipparini, F. Egidi, J. Goings, B. Peng, A. Petrone, T. Henderson, D. Ranasinghe, V.G. Zakrzewski, J. Gao, N. Rega, G. Zheng, W. Liang, M. Hada, M. Ehara, K. Toyota, R. Fukuda, J. Hasegawa, M. Ishida, T. Nakajima, Y. Honda, O. Kitao, H. Nakai, T. Vreven, K. Throssell, J.A. Montgomery Jr., J.E. Peralta, F. Ogliaro, M.J. Bearpark, J.J. Heyd, E.N. Brothers, K.N. Kudin, V.N. Staroverov, T.A. Keith, R. Kobayashi, J. Normand, K. Raghavachari, A.P. Rendell, J.C. Burant, S.S. Iyengar, J. Tomasi, M. Cossi, J.M. Millam, M. Klene, C. Adamo, R. Cammi, J.W. Ochterski, R.L. Martin, K. Morokuma, O. Farkas, J.B. Foresman, D.J. Fox, Gaussian 16 Rev. B.01, (2016).
[34] C.R. Wick, E. Topraksal, D.M. Smith, A.-S. Smith, cogef.py: Tools to run COnstraint Geometries simulate External Force calculations, (2022). 10.5281/ZENODO.7079733.
[35] C.R. Wick, E. Topraksal, D.M. Smith, A.-S. Smith, Evaluating the predictive character of the method of constrained geometries simulate external force with density functional theory, Zenodo - Dataset (2022), https://doi.org/10.5281/ZENODO.6948605 [Dataset].
[36] M. Livraghi, K. Höllring, C.R. Wick, D.M. Smith, A.-S. Smith, An exact algorithm to detect the percolation transition in molecular dynamics simulations of cross-linking polymer networks, J. Chem. Theory Comput. 17 (2021) 6449–6457, https://doi.org/10.1021/acs.jctc.1c00423.
[37] S.N. Zhurkov, V.E. Korsukov, Atomic mechanism of fracture of solid polymers, J. Polym. Sci. Polym. Phys. Ed. 12 (1974) 385–398, https://doi.org/10.1002/pol.1974.180120211.

[38] I.M. Brown, T.C. Sandreczki, Fracture-induced free radicals in amine-cured epoxy resins, Macromolecules 18 (1985) 1041–1043, https://doi.org/10.1021/ma00147a041.
[39] M.A. Grayson, C.J. Wolf, Mechanochemical reactions in an epoxy resin system, J. Polym. Sci. Polym. Phys. Ed. 23 (1985) 1087–1097, https://doi.org/10.1002/pol.1985.180230601.
[40] R.S. Porter, A. Casale, Recent studies of polymer reactions caused by stress, Polym. Eng. Sci. 25 (1985) 129–156, https://doi.org/10.1002/pen.760250302.
[41] G.S. Kedziora, S.A. Barr, R. Berry, J.C. Moller, T.D. Breitzman, Bond breaking in stretched molecules: multi-reference methods versus density functional theory, Theor. Chem. Acc. 135 (2016) 79, https://doi.org/10.1007/s00214-016-1822-z.
[42] M. Tabata, T. Miyazawa, J. Sohma, Direct evidence of main-chain scissions induced by ultrasonic irradlation of benzene solutlons of polymers, Chem. Phys. Lett. 73 (1980) 3, https://doi.org/10.1016/0009-2614(80)85230-4.
[43] C.E. Diesendruck, G.I. Peterson, H.J. Kulik, J.A. Kaitz, B.D. Mar, P.A. May, S. R. White, T.J. Martínez, A.J. Boydston, J.S. Moore, Mechanically triggered heterolytic unzipping of a low-ceiling-temperature polymer, Nat. Chem. 6 (2014) 623–628, https://doi.org/10.1038/nchem.1938.
[44] R. Nixon, G. De Bo, Three concomitant C–C dissociation pathways during the mechanical activation of an N-heterocyclic carbene precursor, Nat. Chem. 12 (2020) 826–831, https://doi.org/10.1038/s41557-020-0509-1.
[45] H.E. Gaub, M. Rief, H. Clausen-Schaumann, Sequence-dependent mechanics of single DNA molecules, Nat. Struct. Biol. 6 (1999) 346–349, https://doi.org/10.1038/7582.